

that of IIIA. The IP and BW values of IIIB are compatible to those of IIIA. Thus, IIIB should have higher intrinsic conductivity than IIIA. Since only doped polyacetylene (ca. 1000 S/cm) provides higher conductivity than IIIA (ca. 500 S/cm),<sup>42</sup> IIIB would be of particular interest in the conducting polymers area.

Both the interring distance ( $d$ ) and the unit cell length ( $l$ ) are smaller in IIIB than in IIIA. This may account for the smaller  $E_g$  value in the former, since smaller  $d$  and  $l$  values would increase the interaction between the basis functions on adjacent rings. Poly( $p$ -pyridine) is another interesting polymer, but it is not calculated here due to its low symmetry. However, one may propose that poly( $p$ -pyridine) should have electronic properties similar to poly( $p$ -phenylene) and poly( $p$ -pyrazine) on the basis of structural considerations.

**D. Class IV Compounds.** Class IV polymers have longer unit cell lengths than their Class III counterparts and  $\pi$  delocalization is less effective in the latter than in the former. As expected, calculated  $E_g$  values for Class IV are much larger than the corresponding Class III polymers. Class IV polymers are then predicted to have much less intrinsic conductivity than their Class III counterparts. Among all Class IV polymers, IVD appears to be of special interest. According to calculations, IVD should have higher intrinsic conductivity than IIIA since a lower  $E_g$  value is obtained for the former (2.2 vs. 2.9 eV). However, the small BW value of IVD may limit its potential applications as a doped polymer. The lower  $E_g$  of IVD clearly demonstrates the capability of S atoms in connecting two unsaturated units as far as conductivity is concerned. This type of capability is deemed to be very important in designing new conducting polymers.

#### Conclusions

We have performed a systematic approach to study four classes (I-IV) of compounds using MOMM and VEH methods. The VEH method achieves its computation speed by evaluating only one-electron integrals and including no self-consistent-field iterative cycles. Hence, a theoretical or experimental structure is a prerequisite to carry out VEH calculations. Since the derivation of structures from the MOMM approach is much faster and is probably more accurate than other similar theoretical tools,<sup>2,3,9,10</sup> the potential benefits of a combination of MOMM and VEH are great. In our opinion, the combination of MOMM and VEH is a powerful tool for screening chemicals prior to their syntheses.

Pitfalls of the current VEH method have been presented and discussed. For certain cases, these pitfalls may lead to a very different interpretation of calculated results, such as polyacene and poly(pyrazinopyrazine). Whether these pitfalls can be avoided by reparametrization of atomic potentials needs to be further explored. The observed pitfalls presented here are in line with those reported in the previous papers by Bredas et al.

Poly( $p$ -pyrazine) and poly( $p$ -pyridine) are predicted to have similar intrinsic conductivities as poly( $p$ -phenylene). As compared with poly( $p$ -phenylene), poly( $p$ -pyrazine) is calculated to be less  $p$ -dopable by acceptors while it is more  $n$ -dopable by donors. Poly(pyridinopyridine) can have two possible spatial arrangements, anti and syn. The anti configuration is calculated to have a lower bandgap than the syn form (0.6 vs. 2.9 eV). Thus, a mixture of syn and anti forms, instead of a pure syn configuration, may be needed to explain the experimentally observed high intrinsic conductivity of poly(pyridinopyridine).

Many interesting features have been revealed through systematic studies and structural analysis. This paper represents an interesting and important extension of previous activities in the influence of molecular architecture on the electronic properties of conducting polymers.<sup>3-8</sup> The -NH- functional group is found to be the most effective in lowering IP values for all cases studied here. This feature may be important in designing  $p$ -dopable polymers. The -S- unit is predicted to be the most effective in lowering the bandgap through decreasing the LUMO (or LUB) energy. Thus, the -S- functional group is a desirable element in designing intrinsic conducting polymers.

**Acknowledgment.** We thank R. Thomson, R. Waugh, and L. Burke for their support and PM internal reviewers for their comments.

**Registry No.** Benzene, 71-43-2; pyridine, 110-86-1; pyrazine, 290-37-9; 1,4-dihydrobenzene, 628-41-1; 1,4-dihydropyrazine, 3026-16-2; 1,4-dioxin, 290-67-5; 1,4-dithiin, 290-79-9; poly(pyridinopyridine), 108167-10-8; poly(pyrazinopyrazine), 95991-23-4; poly(1,4-dihydrobenzo-1,4-dihydrobenzene), 108232-80-0; poly(1,4-dihydropyrazino-1,4-dihydropyrazine), 108232-79-7; poly(1,4-dioxino-1,4-dioxin), 108150-06-7; poly(1,4-dithiino-1,4-dithiin), 108150-08-9; poly( $p$ -phenylene), 25190-62-9; poly( $p$ -pyrazine), 42319-72-2; poly( $p$ -1,4-dihydrobenzene), 33040-25-4; poly( $p$ -1,4-dihydropyrazine), 108150-02-3; poly( $p$ -dioxin), 108150-03-4; poly( $p$ -dithiin), 108150-04-5.

## A Theoretical Study of Thermal Reactions of Bicyclo[2.1.0]pent-2-ene

P. N. Skancke,\*† K. Yamashita, and K. Morokuma\*

Contribution from the Institute for Molecular Science, Myodaiji, Okazaki 444, Japan.  
Received December 2, 1986

**Abstract:** Ab initio molecular orbital calculations, using 3-21G, 6-31G, and 6-31G\* basis sets and including electron correlation through CASSCF and Møller-Plesset calculations up to fourth order, have been applied in a study of the thermal walk rearrangement in bicyclo[2.1.0]pent-2-ene (**1**). On the basis of our calculations and estimates, we conclude that this process occurs with inversion at the migrating center and that it probably is a two-step reaction. The activation energy for this symmetry-allowed walk rearrangement is found to be around 10 kcal/mol higher than that for the symmetry-forbidden disrotatory electrocyclic ring opening leading to cyclopentadiene. Estimates have been made of the influence that an electron-withdrawing substituent on the migrating carbon, the  $\text{—C}\equiv\text{N}$  group, has on the activation energies. It is found that the substitution favors the walk reaction energetically relative to the ring opening, in accordance with experimental findings.

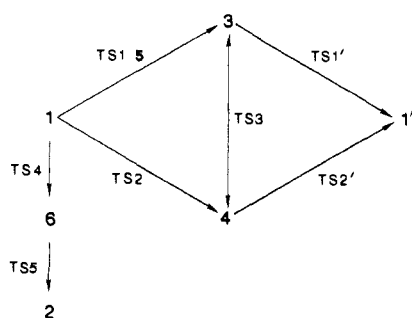
The walk rearrangement, defined as a reaction in which a divalent group such as  $\text{—O—}$ ,  $\text{—NR—}$ , or  $\text{—CR}_2\text{—}$  moves along the surface of a conjugated cyclic  $\pi$ -electron system,<sup>1</sup> is of central importance in the discussion of the predictive power of the

Woodward-Hoffmann symmetry rules.<sup>2</sup> If the rearrangement is a concerted reaction, it may be classified as a sigmatropic process in which orbital symmetry requirements lead to highly stereospecific reaction modes. These rules, applied to the circumam-

\* Permanent address: Department of Chemistry, The University of Tromsø, P.O. Box 953, N-9001, Tromsø, Norway.

(1) Klärner, F.-G. *Topics Stereochem.* **1984**, *15*, 1.  
(2) Woodward, R. B.; Hoffmann, R. *Angew. Chem., Int. Ed. Engl.* **1969**, *8*, 781.

Scheme I



ulation of a  $-\text{CH}_2-$  group in consecutive  $(1,n)$  sigmatropic shifts, predict that the  $(1,3)$  shift goes via inversion of the migrating center for suprafacial processes, whereas the  $(1,5)$  shift goes via retention. In contrast to these symmetry rules, the Berson-Salem rules,<sup>3</sup> based on the assumption of subjacent orbital control, predict retention for the  $(1,3)$  shift and inversion for the  $(1,5)$  shift. For recent reviews of this kind of processes we refer to Childs<sup>4</sup> for circumambulation reactions in general and to Klärner<sup>1</sup> for the more specific walk rearrangements. These reviews also contain exhaustive sets of references.

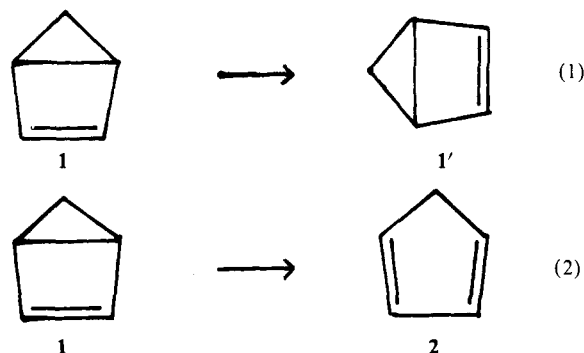
It has been known for some time that several unsaturated five-membered heterocycles undergo a photochemically induced isomerization leading to a redistribution of the ring atoms.<sup>5</sup> In the interpretation of these reactions, walk rearrangements in the valence tautomeric bicyclic heterocompounds, generated as intermediates, have been invoked. It has also been shown that in some derivatives of 5-thiabicyclo[2.1.0]pent-2-ene a fast, thermally induced, walk reaction takes place.<sup>6</sup>

Also in 1,3-cyclopentadiene (2) a redistribution of ring atoms takes place by photolysis.<sup>7</sup> This reaction has been interpreted in terms of a photoinduced walk rearrangement in the hydrocarbon bicyclo[2.1.0]pent-2-ene (1). A thermally induced walk rearrangement in 1 does not compete favorably with the electrocyclic ring opening to 2.<sup>7,8</sup>

The present work was prompted by the extensive and systematic experimental study of Klärner et al.<sup>9</sup> on thermal walk rearrangements in substituted bicyclo[2.1.0]pent-2-enes in solution. They found that in carboxylates and nitriles of the parent compound the walk process competed with the electrocyclic ring opening at room temperature and that the reaction could be observed even at 0 °C. Furthermore it was unambiguously established that the rearrangement was a highly stereospecific one with inversion at the migrating center, in accordance with the Woodward-Hoffmann rules.

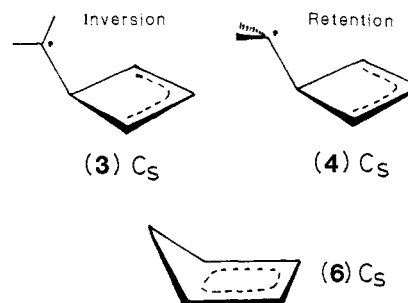
The purpose of the present study is to scrutinize parts of the potential surface for the degenerate process and to compare the energetics of this process with the one of the electrocyclic ring opening. The species that a priori are of interest in the processes referred to are connected in Scheme I.

In the walk process  $1 \rightarrow 1'$  we label as 3 the transient species that occurs if the reaction proceeds with inversion at the migrating center and as 4 the corresponding one with retention at this center. For reasons of symmetry 3 and 4 represent stationary points on the potential surface, being transition states in concerted one-step processes and local minima in case of two-step processes. In the latter case there should be transition states (TS) of  $C_1$  symmetry between 1 and 3, 1 and 4, and 3 and 4, respectively. In the



ring-opening reaction  $1 \rightarrow 2$  the transient species 6 may be a transition state or a local minimum. In the latter case, transition states TS4 and TS5 also occur.

In our calculations, as will be discussed below, we have chosen a  $C_s$  symmetry for 6, giving the following transient species.



To our knowledge only limited studies of reaction (1) have previously been made by theoretical methods. A semiempirical study of 3 and 4 led to the conclusion that 4 was slightly (4 kcal/mol) more stable than 3, giving preference to a retention of the migrating center,<sup>10</sup> in conflict with the HOMO-LUMO symmetry rules and with the experimental findings for derivatives of 1.<sup>9</sup> In a preliminary UHF study by one of us the lowest singlet and triplet states of 3 and 4 were optimized, 3 being found to have the lowest energy.<sup>11</sup> The predicted energy difference was, however, very small (around 2 kcal/mol both for singlets and triplets). The spin densities obtained in the UHF study indicated a biradical character of both 3 and 4. Their vibrational characteristics were not analyzed.

The electrocyclic ring opening (2) of 1 and its methyl derivatives has been extensively discussed, and alternative mechanisms have been suggested.<sup>12,13</sup> A breaking of the bridgehead bond in 1, analogous to the concerted ring opening of cyclobutene, is compelled to occur under  $C_s$  symmetry due to steric constraints and is thus thermally symmetry-forbidden. Alternative mechanisms are nonconcerted cleavage of the bridgehead bond, hydrogen migration in analogy with the cyclopropane-propene isomerization, and a  $(\sigma^2 + \sigma^2a)$  process involving a cleavage of two carbon-carbon bonds.

MINDO/3 calculations<sup>13</sup> on the thermal isomerization of 1 to 2 led to an activation energy for the  $C_s$  path in good agreement with the experimental value of 26.9 kcal/mol.<sup>12b</sup> Furthermore, in a recent study applying MNDO and MINDO/3 calculations

(10) Schoeller, W. W. *J. Am. Chem. Soc.* **1975**, *97*, 1978.

(11) Skancke, P. N. *Croat. Chem. Acta* **1984**, *57*, 1445.

(3) Berson, J. A.; Salem, J. J. *J. Am. Chem. Soc.* **1972**, *94*, 8917.  
 (4) Childs, R. F. *Tetrahedron* **1982**, *38*, 567.  
 (5) Pawda, A. In *Rearrangements in Ground and Excited States*; Academic Press: New York, 1980; Vol. 3, p 501.  
 (6) (a) Ross, J. A.; Seiders, R. P.; Lemal, D. M. *J. Am. Chem. Soc.* **1976**, *98*, 4325. (b) Bushweller, C. H.; Ross, J. A.; Lemal, D. M. *Ibid.* **1977**, *99*, 629.  
 (7) Andrews, G. D.; Baldwin, J. E. *J. Am. Chem. Soc.* **1976**, *98*, 4851, 4853.  
 (8) Gajewski, J. J. *Hydrocarbon Thermal Isomerizations*; Academic Press: New York, 1981.  
 (9) Klärner, F.-G.; Adamsky, F. *Chem. Ber* **1983**, *116*, 299.

(12) (a) Brauman, J. I.; Golden, D. M. *J. Am. Chem. Soc.* **1968**, *90*, 1920. (b) Golden, D. M.; Brauman, J. I. *Trans. Faraday Soc.* **1969**, *65*, 464. (c) Baldwin, J. E.; Pinschmidt, R. K., Jr.; Andrist, A. H. *J. Am. Chem. Soc.* **1970**, *92*, 5249. (d) Baldwin, J. E.; Andrews, G. O. *Ibid.* **1972**, *94*, 1775. (e) Flowers, M. C.; Frey, H. M. *Ibid.* **1972**, *94*, 8636. (f) Brauman, J. I.; Farnett, W. E.; D'Amore, M. D. *Ibid.* **1973**, *95*, 5043. (g) Baldwin, J. E.; Andrist, A. H. *J. Chem. Soc., Chem. Commun.* **1970**, 1561. (h) Andrews, G. D.; Davalt, M.; Baldwin, J. E. *Ibid.* **1973**, *95*, 5044. (i) Andrews, G. D.; Baldwin, J. E. *Ibid.* **1977**, *99*, 4853. (j) McLean, S.; Findlay, D. M.; Dmitrienko, G. I. *J. Am. Chem. Soc.* **1972**, *94*, 1380. (k) Altmann, J. A.; Tee, O. S.; Yates, K. *J. Am. Chem. Soc.* **1976**, *98*, 7132.  
 (13) Dewar, M. J. S.; Kirschner, S. *J. Chem. Soc., Chem. Commun.* **1975**, 461.

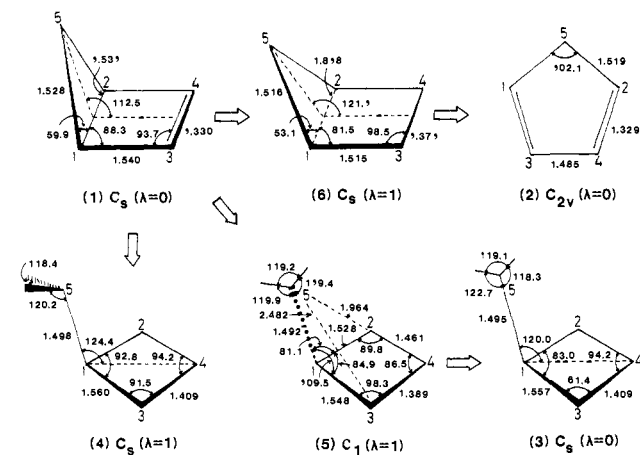


**Figure 1.** Optimized geometries (in Å and deg) at the HF/3-21G level.  $\lambda$  is the number of normal coordinates having imaginary frequencies. Species **1** and **2** have RHF solutions, whereas all the other species give singlet UHF solutions.

**Table I.** Calculated Mulliken Atomic Spin Densities for the Singlet UHF Wave Functions<sup>a</sup>

species	3	4	5	6
C <sub>1</sub>	0.08	0.11	0.16	1.17
C <sub>2</sub>	-1.16	-1.27	-1.03	-1.17
C <sub>3</sub>	-1.16	-1.27	-1.14	-1.18
C <sub>4</sub>	0.95	0.96	1.01	1.18
C <sub>5</sub>	1.41	1.44	1.12	0

<sup>a</sup>At the UHF/3-21G//UHF/3-21G level.

it was found that the thermal rearrangement of bicyclo[2.1.0]pentanone to cyclopentadienone along the path retaining C<sub>s</sub> symmetry had a very low activation energy (MNDO 9.2 kcal/mol, MINDO/3 14.3 kcal/mol).<sup>14</sup> Neither of the two semiempirical studies referred to above presented an analysis of the wavefunction of the transition state.

### Hartree-Fock Calculations

Preliminary Hartree-Fock calculations with analytical first and second derivatives on the ground states of **1**–**6** were performed with the 3-21G basis set, by using the program GAUSSIAN82.<sup>15</sup> In order to treat the systems with closed and open shell electronic structures in a consistent way, we have used the unrestricted HF method. Since the UHF wave functions are not eigenfunctions of S<sup>2</sup> and include contaminations of higher spin states, the stability of the singlet UHF energies are sometimes overestimated. Nonetheless, geometrical structures in which odd electrons are localized far away from each other are reasonably well predicted by the singlet UHF method.<sup>16</sup> More sophisticated methods, CASSCF and UMP, will be used to analyze the nature of the wave functions and the energetics of the systems in the subsequent sections.

A selection of parameters from the completely optimized geometries at this level of calculation are shown in Figure 1. For **1** and **2** RHF solutions were obtained (even if a UHF initial guess were used), whereas for **3** and **4** having open-shell states <sup>1</sup>A' and <sup>1</sup>A'', respectively, UHF wave functions were calculated. These calculations will later be referred to in general as HF calculations. The Mulliken atomic spin distributions obtained for **3** and **4**, given in Table I, confirm their biradical character previously suggested.<sup>11</sup> Calculation of vibrational frequencies at the optimized geometry for **3** gave exclusively real frequencies indicating that this species is a local minimum on the potential surface. A similar analysis for **4** gave one imaginary frequency (134i cm<sup>-1</sup>). This vibrational

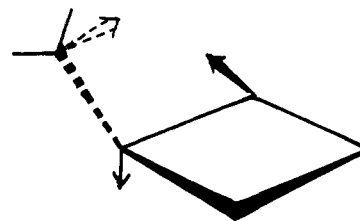
**Table II.** Energies (in kcal/mol) Relative to the Reactant Bicyclo[2.1.0]pent-2-ene (**1**) at Different Levels of Calculation at the HF/3-21G Optimized Geometries

	reactant <b>1</b>	walk		ring opening	
		TS <b>5</b>	intrmdt <b>3</b>	TS <b>6</b>	prod. <b>2</b>
HF/3-21G	-191.621 65 <sup>a</sup>	16.8	4.7	9.8	-59.9
HF/6-31G	-192.621 06	16.8	1.9	8.7	-61.3
HF/6-31G*	-192.708 91	21.6	9.3	13.7	-51.8
CASSCF/3-21G	-191.671 58		23.4		-64.3
MP2/6-31G	-193.063 53	42.2	40.4	33.1	-56.3
MP2/6-31G*	-193.349 86	47.3	51.1	37.9	-45.8
MP3/6-31G	-193.094 32	39.0	35.9	30.0	-55.9
MP3/6-31G*	-193.380 93	42.7	43.7	33.3	-47.1
MP4/6-31G	-193.104 44	36.0	33.8	26.9	-56.7
MP4/6-31G*	-193.388 17	39.4	41.5	30.1	-47.3
experiment				26.88 <sup>b</sup>	-47 <sup>c</sup>

<sup>a</sup>Total energy in hartrees. <sup>b</sup>From ref 12b. <sup>c</sup>From ref 19 and 20. Estimated indirectly. See text.

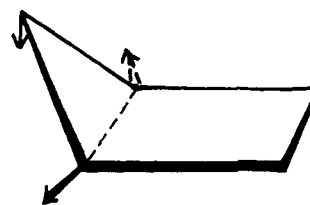
mode of a'' symmetry is mainly a twist of the CH<sub>2</sub> group showing that **4** is a transition state for the conversion of **3** into itself.

The search for a transition state between **1** and **3** led to a species **5** of symmetry C<sub>1</sub> having a singlet UHF solution with atomic spin densities shown in Table I and the geometry given in Figure 1.



The only normal mode with an imaginary frequency (666i cm<sup>-1</sup>) in **5** has main contributions shown above by arrows. They come from the CH<sub>2</sub> group and the terminal carbon of the allylic system being closest to this group and showing that this is the reaction coordinate connecting **1** and the intermediate **3**.

The transition state for the electrocyclic ring opening of **1** was optimized under a constraint of C<sub>s</sub> symmetry. The main geometrical parameters of the resultant species **6** are shown in Figure 1. The structure obtained for **6** deviates significantly from the one predicted previously by MINDO/3 calculations.<sup>13</sup> The main difference between the geometries are the C<sub>1</sub>–C<sub>3</sub> and C<sub>1</sub>–C<sub>5</sub> distances found to be 1.43 and 1.85 Å, respectively, by MINDO/3,<sup>13</sup> compared with the values 1.515 and 1.516 Å, respectively, in the present work. Furthermore the angle between the three- and four-membered ring was predicted to be 135°, substantially larger than our value of 121°. In our calculation species **6** was found to have one imaginary vibrational frequency at 896i cm<sup>-1</sup> confirming that this is a true transition state. The dominating component of this normal mode, shown below, is a motion of the CH<sub>2</sub> group toward the quasi four-membered ring and a stretch of the distance between the bridgehead carbon atoms. This synchronized motion will lead to **2**, thus confirming that this transition state is on the reaction coordinate for the process **1** → **2**.



An important feature of the wavefunction for the transition state **6** is that not only the spin symmetry but also the space symmetry of the molecular orbitals is broken. An extensive HOMO–LUMO mixing took place to give symmetry-broken MOs. The Mulliken atomic spin distribution, shown in Table I, is analogous to the

(14) Schweig, A.; Thiel, W. *J. Comput. Chem.* **1980**, *1*, 129.

(15) Binkley, J. A.; Frisch, M. J.; DeFrees, D. J.; Reghavarachi, K.; Whiteside, R. A.; Schlegel, H. B.; Pople, J. A. GAUSSIAN82, Carnegie Mellon Chemistry Publishing Unit, Pittsburgh 1984.

(16) For example; Yu, J. G.; Fu, X. Y.; Liu, R. Z.; Yamashita, K.; Koga, N.; Morokuma, K. *Chem. Phys. Lett.* **1986**, *125*, 438.

ground-state spin structure obtained by UHF calculations on the cyclobutadiene diradical.<sup>17</sup> Furthermore, this distribution is well adapted for couplings appropriate to both **1** and **2** depending on the geometrical deformation of the transition state.

At the optimized transition state **6** we also obtained an RHF solution and carried through a second-order stability test of its wave function.<sup>18</sup> The RHF energy was found to be 9.5 kcal/mol above the symmetry-broken UHF solution. Furthermore we found this wave function to be unstable relative to a UHF function, the major contributions to the perturbed wave function being orbital pairs all having the symmetry combinations  $a''$ , thus breaking orbital symmetry. This instability, which is a crossing instability,<sup>17</sup> arises from a crossing of the HF states for **1** and **2**.

At this level of calculation we obtained the following energies relative to **1**: **2**, -59.9; **3**, 4.7; **4**, 7.4; **5**, 16.8; and **6**, 9.8 kcal/mol (see also Table II). Qualitatively these data reflect the large exothermicity observed for the ring opening process.<sup>19</sup> For the  $\Delta H_f^\circ$  of **2** there are two experimental values,<sup>20</sup> 31.9 and 32.4 kcal/mol. For **1** there is an indirectly determined value<sup>19</sup> of 79.1 kcal/mol based on the heat of hydrogenation of **1** and  $\Delta H_f^\circ$  of bicyclopentane. This leads to an experimental energy difference between **2** and **1** of around 47 kcal/mol, indicating that the relative energy obtained for **1** at this level of calculation is too high by around 13 kcal/mol. A further indication of the inappropriateness of this energy are the low values predicted for the activation energies. The activation energy for the electrocyclic ring opening **1**  $\rightarrow$  **2** has been determined experimentally in the vapor phase<sup>12b</sup> and is found to be  $26.88 \pm 0.32$  kcal/mol. The corresponding energy for the walk rearrangement has to be substantially higher, as this process is unable to compete with the ring opening of the unsubstituted hydrocarbon **1**.<sup>8</sup> For ester and nitrile derivatives of **1**, activation energies for the walk process in solution have been found to be around 22–25 kcal/mol.<sup>9</sup>

#### CASSCF Calculations

In order to obtain more realistic characteristics of the electronic structures of reactant, products, and transient species, calculations beyond the HF approximation were carried through. Except for cases that will be discussed below, the geometries assumed were those obtained by optimizations at the HF level by using the 3-21G basis.

In the CASSCF calculations, carried through with the program GAMESS,<sup>22</sup> the active space was limited to four electrons and four orbitals. In  $C_s$  symmetry all the species will have two  $a'$  and two  $a''$  active orbitals leading to 12 singlet configurations of  $A'$  symmetry. The natural choice of orbitals for the ring opening process is the following: in **2** the four  $\pi$ -orbitals and in **1** the two  $\pi$ -orbitals and the two transannular orbitals ( $\sigma$  and  $\sigma^*$ ). For the transition state **6** having  $C_s$  symmetry the correlation of the "correct" electron pairs localized around the bridgehead carbons is difficult within the four active orbital scheme, as the transannular region has been depleted of electrons (bond population 0.0038 at the HF level), and calculation led to correlation of electron pairs constituting bonding to the  $CH_2$  group. Therefore, we did not carry through CASSCF calculation for **6**.

For the study of the walk rearrangement, we have correlated the three ring  $\pi$ -orbitals and the  $CH_2$  p orbital for **3**. To be consistent, we would have to correlate the two  $\pi$ -electrons and the electrons in one of the side bonds of the three-membered ring in **1**. This would have led to a situation where the reference state for **1**, denoted by **1a** below, would be different for the two competing processes studied. For the transition state **5** having  $C_1$

**Table III.** Mulliken Bond Overlap Population in Bicyclo[2.1.0]pent-2-ene (**1**) Calculated by Different Basis Sets<sup>a</sup>

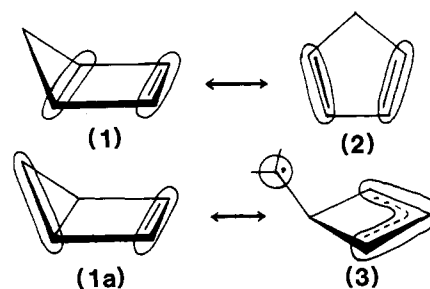
method	bond			
	1-2	1-3	1-5	3-4
RHF/3-21G	0.1058	0.3009	0.0634	0.5175
RHF/6-31G	0.1549	0.3436	0.1060	0.6489
RHF/6-31G*	0.2735	0.3835	0.2416	0.6945

<sup>a</sup>Labeling of atoms in Figure 1. The geometry optimized at the RHF/3-21G level.

**Table IV.** Mulliken Bond Overlap Populations in the Intermediate **3** Calculated by Different Basis Sets

method	bond			
	1-2	1-5	2-4	2...5
UHF/3-21G//UHF/3-21G	0.3054	0.2144	0.3952	-0.0900
UHF/6-31G//UHF/3-21G	0.3281	0.2285	0.4755	-0.0674
UHF/6-31G*//UHF/3-21G	0.2982	0.2982	0.5193	-0.0487
UHF/6-31G*//UHF/6-31G*	0.3605	0.3002	0.5258	-0.0456
UMP/3-21G//UMP2/3-21G	0.3123	0.2016	0.3917	-0.0945

<sup>a</sup>Labeling of atoms in Figure 1.



symmetry it is not possible to define a four orbital active space that is consistent with the one chosen above. Accordingly CASSCF calculations for this species were not carried through. These inconsistencies for **1a**, **5**, and **6** can only be removed by expanding the active space to eight electrons and eight orbitals, leading to computations that are too demanding. However, the four electrons/four orbitals CASSCF calculations carried through for **1-3** gave some valuable information on their electronic structures.

The CASSCF wave functions for **1** and **2** confirmed the closed-shell nature of these molecules by coefficients of 0.979 and 0.967 for the doubly occupied ground configurations,  $\dots(12a')^2(6a'')^2$  and  $\dots(11a')^2(7a'')^2$ , respectively. For **1** the only additional configuration with coefficient larger than  $|0.1|$  is the  $^1A'$  function  $\dots(11a')^1(12a')^1(7a'')^1(8a'')^1$  having the value -0.119. In the case of **2** the corresponding configuration  $\dots(10a')^1(8a'')^1(11a')^1(9a'')^1$  has the value -0.154. Here also  $\dots(8a'')^2(11a')^2$  contributes by -0.146. For the transient species **3** the dominating configuration is  $\dots(13a')^2(5a'')^1(6a'')^1$  with the coefficient 0.858. Here the largest closed shell contribution comes from the configuration  $\dots(13a')^2(5a'')^2$  with coefficient -0.294, which is smaller than the value of -0.348 for the configuration  $\dots(13a')^1(5a'')^1(6a'')^1(14a')^1$ .

The energy lowerings relative to HF energies obtained by the CASSCF calculations were 31.3, 35.7, and 12.6 kcal/mol for **1**, **2**, and **3**, respectively. As shown in Table II, this results in a larger energy difference between the closed shell molecules **1** and **2** than the one predicted by HF calculations, thus making the discrepancy with experiment larger. The relative lowering brings the intermediate **3** around 20 kcal/mol higher relative to **1** than predicted at the HF level.

#### Møller-Plesset Calculations

As a substitute for large scale MCSCF and additional CI calculations, we carried out Møller-Plesset (MP) calculations<sup>23</sup>

(17) Fukutome, H. *Int. J. Quantum Chem.* **1981**, *20*, 955.

(18) Seeger, R.; Pople, J. A. *J. Chem. Phys.* **1977**, *66*, 3045.

(19) Roth, W. R.; Klärner, F.-G.; Lennartz, H.-W. *Chem. Ber.* **1980**, *113*, 1818.

(20) See: discussion in Olivella, S.; Urgi, F.; Vilanasa, J. *J. Comput. Chem.* **1984**, *5*, 230.

(21) Andrews, G. D.; Baldwin, J. E.; Gilbert, K. E. *J. Org. Chem.* **1980**, *45*, 1523.

(22) Dupuis, M.; Spangler, D.; Wendoloski, J. J. NRCC Software Catalog, Vol. 1, Program GG01 (GAMESS), 1980.

(23) Møller, C.; Plesset, M. S. *Phys. Rev.* **1934**, *46*, 618. Pople, J. A.; Binkley, J. S.; Seeger, R. *Int. J. Quantum Chem. Symp.* **1976**, *10*, 1.

**Table V.** Mulliken Bond Overlap Populations in the Transition State **5** Calculated by Different Basis Sets

basis	bond <sup>a</sup>						
	1-2	1-3	1-5	2-4	2...5	3-4	3...5
UHF/3-21G//UHF/3-21G	0.3004	0.2382	0.1584	0.3355	-0.0967	0.4267	-0.1134
UHF/6-31G//UHF/3-21G	0.3480	0.2731	0.1807	0.3873	-0.0513	0.5219	-0.0855
UHF/6-31G*//UHF/3-21G	0.3788	0.3299	0.2706	0.4382	0.0171	0.5639	-0.0570
UHF/6-31G*//UHF/6-31G*	0.3825	0.3310	0.2730	0.4497	-0.0023	0.5640	-0.0530
UMP/3-21G//UMP2/3-21G	0.3107	0.2737	0.1750	0.3630	-0.1547	0.4088	-0.1047

<sup>a</sup> Labeling of atoms in Figure 1.**Table VI.** Energies of Transition State **5** and Intermediate **3** for Walk Rearrangement at Advanced Levels of Calculation

geometry	optmztn	energy	transtn state <b>5</b> <sup>a</sup>	intrmdt <b>3</b> <sup>b</sup>
HF/6-31G*	HF/6-31G*		+12.2	-192.695 46
	MP2/6-31G*		-2.7	-193.269 83
MP2/3-21G	HF/3-21G		+8.9	-191.612 78
	MP2/3-21G		+4.3	-192.006 74
	HF/6-31G*		+9.7	-192.692 04
	MP2/6-31G*		+2.9	-193.268 58

<sup>a</sup> Energy relative to **3** in kcal/mol. <sup>b</sup> Total energy in hartrees.

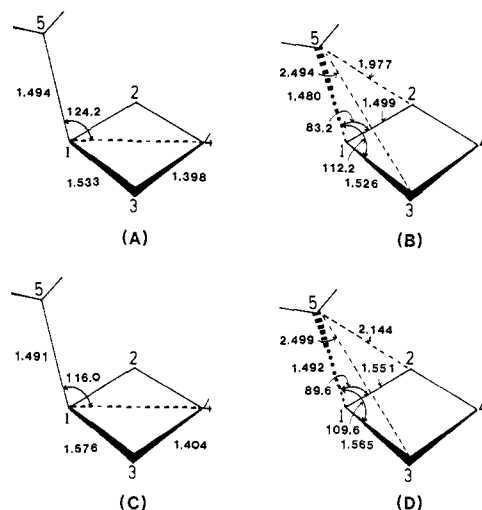
up to fourth order and by using different basis sets. Reference wave functions used for MP calculations are the stable HF solutions for the respective species: RHF for **1** and **2**, UHF for **3** and **5**, and broken-symmetry UHF for **6**. Except for cases discussed below HF/3-21G optimized geometries were assumed. The fourth-order calculations included single, double, and quadruple excitations. Relative energies obtained at different levels of calculation are given in Table II where also experimental energies are found. Mulliken population analysis for **1**, **3**, and **5** gives the results shown in Tables III, IV, and V, respectively.

The data in Table II show that the energy difference between the closed shell molecules **1** and **2** is rather insensitive to the order of perturbation applied. They do, however, change significantly when d-orbitals are included in the basis. This change brings the calculated energy difference into reasonable agreement with the experimental one of 47 kcal/mol and is the result of a stabilization of **1** by d-orbital participation in the bonding regions, particularly around the bridgehead carbons. A quantitative picture of the increased bonding is given by the data in Table III. It is noted that the overlap populations in the transannular bonding region 1-2 and in the side bond 1-5 of the three-membered ring are substantially increased by d-orbital participation.

The relative energy for the intermediate **3** is increased by about the same amount as for **2** when d-orbitals are included, reflecting the stabilization of **1**. Here the picture is more complex as this energy also depends strongly on the level of calculation, the decisive jump being from HF to MP2. In going from MP2 to MP4 the energy decreases by 7-10 kcal/mol for both basis sets.

The relative energies of **3** and **5** are important for the description of the walk rearrangement as a concerted process or a two-step process having a diradical intermediate. These energies therefore deserve some further comments.

The basis set dependence of the energy difference between **3** and **5**, although noticeable, is completely submerged in the large change found by going from HF to MP calculations. The data in Table II show that this energy difference is decreased to a very small amount at the MP level and that it is virtually independent of the order of perturbation. At this level of calculation the basis set dependence of the energies therefore becomes important. Inclusion of d-functions brings **5** below **3** in energy at all levels of MP calculations. Considering the fact that the energy differences are very small and that the number of independent structural parameters in these systems is large, a reoptimization of the geometries at the MP level using an augmented basis set could probably reverse the ordering. Ideally MP2/6-31G\* optimizations would be desirable. Such calculations are however too costly. In order to obtain an estimate of the effect of geometry optimization on the MP energetics, we calculated  $\Delta E = E_5 - E_3$  by using MP2/6-31G\* at geometries optimized by HF/6-31G\* and MP2/3-21G, respectively. Some of the geometrical param-

**Figure 2.** Optimized geometries (in Å and deg) at the HF/6-31G\* (A and B) and the MP2/3-21G level (C and D) for **3** and **5**.

eters are shown in Figure 2, the energetics in Table VI, and population in Table IV and V. The value of  $\Delta E$  for MP2/6-31G\*//MP2/6-31G\* was then estimated by using the additivity approximation

$$\begin{aligned} \Delta E(\text{MP2/6-31G}^*//\text{MP2/6-31G}^*) &\approx \\ &\Delta E(\text{MP2/6-31G}^*//\text{HF/6-31G}^*) - \\ &\Delta E(\text{MP2/6-31G}^*//\text{HF/3-21G}) + \\ &\Delta E(\text{MP2/6-31G}^*//\text{MP2/3-21G}) = \\ &(-2.7) - (-3.8) + (+2.9) = +4.0 \end{aligned}$$

From this relation a value of +4.0 kcal/mol was found. Another additivity approximation would give an estimate for the best calculation  $\Delta E(\text{MP4/6-31G}^*//\text{MP2/6-31G}^*)$  to be around +5.7 kcal/mol.

$$\begin{aligned} \Delta E(\text{MP4/6-31G}^*//\text{MP2/6-31G}^*) &\approx \\ &\Delta E(\text{MP2/6-31G}^*//\text{MP2/6-31G}^*) - \\ &\Delta E(\text{MP2/6-31G}^*//\text{HF/3-21G}) + \\ &\Delta E(\text{MP4/6-31G}^*//\text{HF/3-21G}) = \\ &(+4.0) - (-3.8) + (-2.1) = +5.7 \end{aligned}$$

Zero-point vibrational energies obtained from HF/3-21G//HF/3-21G calculations, 57.1 and 58.3 kcal/mol for **3** and **5**, respectively, will give a vibrationally corrected energy difference of +5.2 to +6.9 kcal/mol. Although this energy difference is small, we may conclude that the walk rearrangement is likely to be a two-step process passing through an intermediate having diradical character.

In order to gain further information on the characteristics of **5** and **3**, we carried through additional calculations as shown below. The transition state **5**, which is geometry optimized at the HF/3-21G level to  $C_1$  symmetry, has negative overlap populations for both the 2...5 and 3...5 regions in a description using s,p-basis sets, as shown in Table V. When d-orbitals are included, the region 2...5, having the shortest of these two  $\text{CH}_2$ -allylic carbon distances, obtains a positive overlap population. This might imply that reoptimizations using an extended basis and a correlated wave function could bring the transition state closer to a structure having  $C_s$  symmetry. The most significant changes obtained by the

**Table VII.** Energies (in kcal/mol) of Nitrile Derivatives of **2**, **3**, **5**, and **6** Relative to Exo and Endo Forms of Bicyclo[2.1.0]pent-2-ene-5-carbonitrile<sup>a</sup>

	walk rearrangement		ring opening	
	TS <b>5</b>	intrmdte <b>3</b>	TS <b>6</b>	prod. <b>2</b>
<b>1</b>	39.4	41.5	30.1	-47.3
<i>exo</i> -CN- <b>1</b>	34.4	34.5	31.0	-44.1
<i>endo</i> -CN- <b>1</b>	35.0	34.2	29.6	-46.1
experiment	(22-25) <sup>b</sup>			

<sup>a</sup>Energies are calculated as corrections to the MP4/6-31G\*/HF/3-21G energies of the parent hydrocarbon species. <sup>b</sup>From ref 9. In solution.

**Table VIII.** Mulliken Bond Overlap Population in **1** and in the Endo and Exo Forms of the Carbonitrile<sup>a</sup>

	bond			
	1-2	1-3	1-5	3-4
<b>1</b>	0.1058	0.3009	0.0635	0.5175
<i>exo</i> -CN- <b>1</b>	0.1180	0.3099	0.0175	0.5129
<i>endo</i> -CN- <b>1</b>	0.1137	0.2900	-0.0053	0.5124

<sup>a</sup>RHF/3-21G at the optimized geometry for **1** (see text).

reoptimizations can be seen from Figure 2. It is seen that the UHF optimization leads to a tighter binding of the carbon atoms in the ring of both **3** and **5** as compared to the geometries given in Figure 1. The relative magnitude of the parameters showing the asymmetry of **5** does not change to any significant extent. In the UMP optimization, however, the difference between the angles C<sub>5</sub>C<sub>1</sub>C<sub>2</sub> and C<sub>5</sub>C<sub>1</sub>C<sub>3</sub> is reduced from around 29° to around 20° indicating a structure closer to C<sub>s</sub> symmetry. Concomitantly, the difference between the nonbonding distances 5...3 and 5...2 is reduced from 0.52 to 0.36 Å. However, the reoptimization of **5** at the HF/6-31G\* and UMP/3-21G levels led to a final structure of C<sub>1</sub> symmetry having the same orientation of the CH<sub>2</sub> group relative to the four-membered ring. The overlap populations obtained for the regions 2...5 and 3...5 in the final structures were -0.0023 and -0.0530, and -0.1547 and -0.1047, respectively. The Hessian of all these final structures **5** has one negative eigenvalue. The corresponding eigenvector has major contributions from the parameters describing the transition from **1** to **3**. This supports the conclusion reached above on the basis of calculated and estimated energy differences.

#### Qualitative Analysis of Substituent Effects

As mentioned above the thermal walk rearrangement in **1** is only observed for certain derivatives of this hydrocarbon. The substituents used at the migrating center in the experimental work of Klärner et al.<sup>9</sup> are the electron-accepting groups —CO<sub>2</sub>CH<sub>3</sub> and —C≡N. In order to obtain an estimate of the possible effects of such groups on the reactivity of **1**, we have made HF/3-21G calculations on the nitrile-substituted hydrocarbons. In these calculations we assumed the HF/3-21G optimized geometries for the parent hydrocarbons and used C—CN and C≡N distances as found by a 3-21G optimization of N≡C—CH<sub>3</sub>. The —C≡N moiety was assumed linear, and its orientation relative to the hydrocarbon was assumed to be the same as for the hydrogen replaced.

As has been discussed and shown in Table II, energy differences obtained by HF/3-21G calculations for the systems involved here are far from being accurate. However, in order to get a qualitative picture of the energetic changes caused by substitution, we have added the energy corrections obtained in such calculations to the presumably best set of energies (MP4/6-31G\* in Table II) for the parent hydrocarbons.

By substitution all species except **2** will have inequivalent endo and exo forms. We have calculated all the forms, and the relative energies are given in Table VI where corresponding energies for the parent hydrocarbons are included for comparison.

The data in Table VII show that a nitrile substitution on the migrating center leads to a lowering of the relative energies for

**3** and **5** whereas **6** is virtually unaffected. This implies a lower activation energy and a higher reaction rate for the walk reaction relative to the corresponding process in the pure hydrocarbon. Although the activation energy for this process still is higher than the one predicted for the electrocyclic ring opening, the change in relative magnitudes is in harmony with experimental results.<sup>9</sup>

As seen from the data in Table VIII the nitrile group induces a pronounced decrease in the 1-5 overlap population both for the endo and for the exo form as compared to the unsubstituted hydrocarbon **1**. This effect is the same as the one experienced in correspondingly substituted cyclopropanes and which is interpreted in terms of charge transfer from the component of the degenerate (e') orbital in cyclopropane having the appropriate symmetry, to the electron-accepting substituent.<sup>24</sup> The concomitant increase in the population of the 1-2 region, observed through bond shortening in cyclopropane, is vanishingly small in **1**. This implies that electron-withdrawing groups at the C<sub>5</sub> position would make the breaking of the 1-5 bond easier than in the parent hydrocarbon but would not change the situation for the 1-2 bond. Thus these results are in conformity with our energy predictions discussed above and with the observed preference for the walk reaction as compared to the ring opening process if electron-accepting groups are attached to the migrating center in **1**. A corresponding study of the electron populations in the unsubstituted transition state **5** and its endo and exo derivatives does not reveal any significant changes in bond populations. However, the gross charge of the migrating carbon atom is reduced by substitution (from 6.34 to 6.13) leading to a stabilization of the diradical. Thus a qualitative interpretation of the observed increase in the walk reactivity, induced by electron-withdrawing substituents, would be in terms of a combined effect, a destabilization of **1** through a bond order decrease in the 1-2 region and a stabilization of the diradical transition state **5** by conjugation. In the intermediate **3** the population analysis shows the same trend as in **5**. Here the change in gross charge at the migrating carbon is from 6.34 in the hydrocarbon to 6.07 in the endo and 6.06 in the exo form of the derivative. The energy difference between the transition state **5** and the intermediate **3** is decreased by 2-3 kcal/mol, suggesting that the ring opening of CN— substituted bicyclo[2.1.0]pent-2-ene might be concerted. A more careful study would be needed to determine unequivocally whether the ring opening is concerted or not.

#### Conclusions

On the basis of the results obtained by our calculations we arrive at the following conclusions. (1) The thermal walk rearrangement in bicyclo[2.1.0]pent-2-ene goes via inversion at the migrating center. (2) The rearrangement is likely a two-step process passing through a diradical intermediate, the transition state being around 5-7 kcal/mol above the intermediate. (3) MP4/6-31G\* calculations reproduce the experimental value for the stability of bicyclo[2.1.0]pent-2-ene relative to cyclopentadiene (calcd 47.3 kcal/mol, experimental 47 kcal/mol), and give a reasonably good agreement with the measured activation energy for the ring opening (calcd 30.1 kcal/mol, experimental 26.9 kcal/mol). (4) The activation energy for the symmetry-allowed walk reaction is about 10 kcal/mol above that for the symmetry-forbidden disrotatory ring opening. (5) An electron-accepting substituent (—C≡N) on the migrating center lowers the activation energy for the walk process but does not change the barrier to disrotatory ring opening.

**Acknowledgment.** One of us (P.N.S.) thanks the Institute for Molecular Science for facilities placed at his disposal and for hospitality enjoyed during the period this work was carried out. He would also like to thank Norges almenvitenskapelige forskningsråd for financial support. Numerical calculations were carried out at the IMS Computer Center.